



**HAL**  
open science

## Mangroves and shoreline erosion in the Mekong River delta, Viet Nam

Manon Besset, Nicolas Gratiot, Edward J. Anthony, Frederic Bouchette, Marc Goichot, Patrick Marchesiello

► **To cite this version:**

Manon Besset, Nicolas Gratiot, Edward J. Anthony, Frederic Bouchette, Marc Goichot, et al.. Mangroves and shoreline erosion in the Mekong River delta, Viet Nam. *Estuarine, Coastal and Shelf Science*, 2019, 226, pp.106263. 10.1016/j.ecss.2019.106263 . hal-02352939

**HAL Id: hal-02352939**

**<https://hal.umontpellier.fr/hal-02352939>**

Submitted on 25 Oct 2021

**HAL** is a multi-disciplinary open access archive for the deposit and dissemination of scientific research documents, whether they are published or not. The documents may come from teaching and research institutions in France or abroad, or from public or private research centers.

L'archive ouverte pluridisciplinaire **HAL**, est destinée au dépôt et à la diffusion de documents scientifiques de niveau recherche, publiés ou non, émanant des établissements d'enseignement et de recherche français ou étrangers, des laboratoires publics ou privés.



Distributed under a Creative Commons Attribution - NonCommercial 4.0 International License

## Mangroves and shoreline erosion in the Mekong River delta, Viet Nam

Manon Besset<sup>a,b,\*</sup>, Nicolas Gratiot<sup>c,d</sup>, Edward J. Anthony<sup>a,e</sup>, Frédéric Bouchette<sup>a</sup>, Marc Goichot<sup>f</sup>,  
Patrick Marchesiello<sup>g</sup>

<sup>a</sup> *University of Montpellier, Geoscience Montpellier, Montpellier, France*

<sup>b</sup> *Aix Marseille University, CNRS, IRD, INRA, Coll France, CEREGE, Aix-en-Provence, France*

<sup>c</sup> *CARE, Ho Chi Minh City University of Technology, VNU-HCM, Viet Nam*

<sup>d</sup> *Université Grenoble Alpes, CNRS, IRD, Grenoble INP, IGE, F-38000 Grenoble, France*

<sup>e</sup> *USR LEEISA, CNRS, Cayenne, French Guiana*

<sup>f</sup> *Lead, Water, WWF Greater Mekong Programme, 14B Ky Dong Street, Ward 9, District 3, Ho Chi Minh, Viet Nam*

<sup>g</sup> *IRD, LEGOS, 14 Avenue Edouard Belin, 31400 Toulouse, France.*

\* *besset@cerege.fr*

### Abstract

The question of the rampant erosion of the shorelines rimming the Mekong River delta has assumed increasing importance over the last few years. Among issues pertinent to this question is how it is related to mangroves. Using high-resolution satellite images, we compared the width of the mangrove belt fringing the shoreline in 2012 to shoreline change (advance, retreat) between 2003 and 2012 for 3687 cross-shore transects, spaced 100 m apart, and thus covering nearly 370 km of delta shoreline bearing mangroves. The results show no significant relationships. We infer from this that, once erosion sets in following sustained deficient mud supply to the coast, the rate of shoreline change is independent of the width of the mangrove belt. Numerous studies have shown that: (1) mangroves promote coastal accretion where fine-grained sediment supply is adequate, (2) a large and healthy belt of fringing mangroves can efficiently protect a shoreline by inducing more efficient dissipation of wave energy than a narrower fringe, and (3) mangrove removal contributes to the aggravation of ongoing shoreline erosion. We fully concur, but draw attention to the fact that mangroves cannot accomplish their land-building and coastal protection roles under conditions of a failing sediment supply and prevailing erosion. Ignoring these overarching conditions implies that high expectations from mangroves in protecting and/or stabilizing the Mekong delta shoreline, and eroding shorelines elsewhere, will meet with disappointment. Among these false expectations are: (1) a large and healthy mangrove fringe is sufficient to stabilize the (eroding) shoreline, (2) a reduction in the width of a large mangrove fringe to the benefit of other activities, such as shrimp-farming, is not deleterious to the shoreline position, and (3) the effects of human-induced reductions in sediment supply to the coast can be offset by a large belt of fringing mangroves.

*Keywords:* Mangroves, Mekong River delta, shoreline erosion, coastal squeeze, sediment supply

## 1    **1.     Introduction**

2           Mangroves are halophytic (tolerant to saline waters) coastal forests that develop at the interface  
3 between muddy shores and mostly brackish waters. Mangroves are characteristic of many tropical and  
4 subtropical coastlines between 32°N and 38°S (Brander et al., 2012). An ecosystem in its own right,  
5 mangroves shelter various fauna, and the thriving and survival of which are totally dependent on healthy  
6 mangroves. A wide and healthy belt of mangroves fringing the shoreline also plays a significant role in  
7 contributing to coastal protection by dissipating waves under normal energetic ocean forcing conditions.  
8 This protective role has been demonstrated in several studies conducted theoretically (Massel et al.,  
9 1999), in the laboratory (Hashim and Catherine, 2013), and from field monitoring (Mazda et al., 1997;  
10 Quartel et al., 2007; Barbier et al., 2008; Horstman et al., 2014), but also from geomorphological and  
11 coastal management-oriented approaches (Anthony and Gratiot, 2012; Winterwerp et al., 2013; Phan et  
12 al., 2015). The protective role of mangroves during the course of extreme climatic and tsunami events  
13 and disasters has been underlined (e.g., Alongi, 2008; Gedan et al., 2011; Marois and Mitsch, 2015).  
14 Mangroves are closely linked with their physical environment and contribute to land-building by trapping  
15 sediment through their complex aerial root structure (e.g., Carlton, 1974; Kathiresan, 2003; Anthony,  
16 2004; Corenblit et al., 2007; Kumara et al., 2010). By contributing to delta aggradation, mangroves  
17 mitigate sea-level rise effects induced by climate change, which in turn are a threat to this ecosystem  
18 (Gilman et al., 2007; McKee et al., 2007; Gedan et al., 2011; Woodroffe et al., 2016). Healthy mangroves  
19 can trap more than 80% of incoming fine-grained sediment (Furukawa et al., 1997) and contribute to  
20 sedimentation rates of the order of 1-8 mm/year, generally higher than local rates of mean sea-level rise  
21 (Gilman et al., 2006; Gupta, 2009; Horstman et al., 2014).

22           On coasts characterized by mangroves, resilience to high-energy events such as tsunami or  
23 repeated storms can be impaired where mangrove loss has been generated and sustained by human  
24 activities. This can be envisaged through consideration of the concept of the tipping point, which  
25 corresponds to a threshold value beyond which a system cannot return to its original dynamic equilibrium  
26 (Kéfi et al., 2016). Tipping points occur where one or more of the driving processes go beyond a  
27 threshold, resulting in destabilized dynamic feedback loops that link all processes together. This can be  
28 expected where the sediment supply is drastically reduced (sediment trapping by dams, sand mining,  
29 etc.), or where oceanic forcing is modified over a long period of time (18.6-year tidal cycles, ocean  
30 oscillations, etc.). This is also the case where a mangrove fringe is reduced in width by coastal ‘squeeze’  
31 or by deforestation (Lewis, 2005; Anthony and Gratiot, 2012). Coastal squeeze occurs where  
32 anthropogenic modifications on the coast lead to a significant cross-shore reduction of coastal space  
33 (Doody, 2004; Pontee, 2013; Torio and Chmura, 2013). A number of case studies have shown that  
34 coastal squeeze can lead to coastal erosion, including in areas where mangroves occur (e.g.,  
35 Heatherington and Bishop, 2012; Anthony and Gratiot, 2012; Winterwerp et al., 2013; van Wesenbeeck  
36 et al., 2015; Toorman et al., 2018; Brunier et al., 2019). van Wesenbeeck et al. (2015) have highlighted  
37 mangrove sensitivity to human pressures and the feedback effects resulting from conversion of mangrove  
38 lands to intensive aquaculture that generates coastal erosion. This leads to a breakdown of the buffer

39 effect of the mangrove forest on wave energy and in promoting sediment trapping. This alteration can  
40 encourage accelerated erosion (Mitra, 2013). In addition, in the case of aquaculture and agriculture, the  
41 river channels commonly become disconnected from the natural floodplain to the benefit of farming,  
42 which results in a significant reduction of sediment supply to the floodplain. A particularly overlooked  
43 area in gauging the significance of mangroves is that of adequate sediment supply, an overarching  
44 background factor without which the commonly considered 'land-building' role of mangroves cannot be  
45 successful. Mangroves are limited producers of sediment (organic or authigenic production), whereas the  
46 negative effects of the reduction of allogenic sediment supply by rivers caused by trapping by dam  
47 reservoirs and by sand mining are often aggravated by accelerated subsidence and sea-level rise. Both  
48 create accommodation space that then requires more sediment to maintain mangrove substrate elevations.

49 The Mekong delta in Viet Nam (Fig. 1), the third largest delta in the world (Coleman and Huh,  
50 2004), has a particularly well-developed mangrove environment (Veettil et al., 2019). The delta makes up  
51 for 12 % of the country's natural land and 19 % of its national population, and hosts a population of 20  
52 million inhabitants (Mekong River Commission, 2010). The delta is crucial to the food security of  
53 Southeast Asia, and provides 50% of Viet Nam's food (General Statistics Office of Viet Nam) and is part  
54 of a river with the most concentrated fish biodiversity per unit area of any large river basin in the world,  
55 with 454 fish species in the delta alone (Vidthayanon, 2008), and ranking second only to the Amazon in  
56 overall biodiversity (WWF, 2012). As the country's largest agricultural production centre, the delta  
57 region contributes half of Viet Nam's rice output, 65 percent of aquatic products and 70 percent of fruits.  
58 It also accounts for 95 percent of the country's rice exports and 60 percent of total overseas shipment of  
59 fish. Following the ravages of the Viet Nam War (1960-1972) on the delta's forests, these important  
60 advantages have significantly impacted the mangroves of the delta, notably in the muddy southwestern  
61 and Gulf of Thailand areas where large tracts have been removed to provide timber for charcoal and for  
62 the construction industry, and to make place for shrimp farms and aquaculture (Phan and Hoang, 1993;  
63 Christensen et al., 2008; Veettil et al., 2019). Several recent studies have also shown that erosion is  
64 becoming increasingly rampant along much of the delta shoreline (Anthony et al., 2015; Besset et al.,  
65 2016; Allison et al., 2017; Li et al., 2017), leading to the recurrent displacement of coastal populations  
66 (Boateng, 2012) and increasing recourse to coastal protection structures, notably dykes (Albers and  
67 Schmitt, 2015). Sea dykes are being increasingly built along parts of the muddy East Sea and Gulf of  
68 Thailand coasts for protection from marine flooding and for shrimp farms, generating a process of  
69 'mangrove squeeze' (Phan et al., 2015).

70  
71 The erosion of the Mekong delta has been attributed to sediment depletion associated with three  
72 main factors (Anthony et al., 2015): (1) potential trapping of sediment by the increasing number of dams  
73 constructed in the Mekong catchment, (2) large-scale commercial sand mining in the river and delta  
74 channels, and (3) accelerated subsidence due to groundwater pumping. With regards to the first two  
75 factors, recent studies have documented a marked reduction in the sediment load of the Mekong River  
76 reaching the delta from 160 Mt/yr in 1990 to 75 Mt/yr in 2014 (Koehnken, 2014), and maybe even down

77 to 40 ±20 Mt/yr currently (Piman and Shrestha, 2017; Ha et al., 2018). This reduction also generates  
78 mechanisms of sediment redistribution by waves and currents that could explain exacerbated shoreline  
79 erosion in places (Marchesiello et al., 2019). 38% of the Mekong delta region is at risk of being  
80 underwater by the year 2100 ([https://en.vietnamplus.vn/forum-to-talk-climateresilient-development-in-](https://en.vietnamplus.vn/forum-to-talk-climateresilient-development-in-mekong-delta/145888.vnp)  
81 [mekong-delta/145888.vnp](https://en.vietnamplus.vn/forum-to-talk-climateresilient-development-in-mekong-delta/145888.vnp)), with a large contribution to this from subsidence generated by massive  
82 groundwater extraction (Minderhoud et al., 2017). Anthony et al. (2015) also suggested, however, that  
83 marked alongshore variability in erosion rates may also be influenced by differences arising from the  
84 presence and protective role of mangroves, or their absence which may enhance erosion. Mangrove loss  
85 thus comes out as an additional factor in modulating erosion of the Mekong delta. Phan et al. (2015)  
86 showed that dissipation of waves incident on the delta shoreline was not effective where mangroves had  
87 been removed, especially in the case of infragravity waves which require a large mangrove cover several  
88 hundred metres wide to be significantly attenuated, such that mangrove removal indeed contributed to  
89 shoreline erosion. On the basis of 18 individual cross-shore profiles distributed along about 320 km of  
90 deltaic coast from the mouths of the Mekong to Ca Mau Point (Fig. 1), Phan et al. (2015) showed a net  
91 correlation between mangrove width and local erosion or accretion. Notwithstanding their limited  
92 number of data points and the large error bars of these points, Phan et al. (2015) identified a minimum  
93 critical width of 140 m for a stable mangrove fringe, and, above this minimum width, a capacity to  
94 promote sedimentation. The authors considered that the larger the width of the mangrove fringe the more  
95 efficient the attenuation of waves and currents will be, offering a successful environment for both  
96 seedling establishment and sedimentation. Indeed, this relationship is in agreement with numerous  
97 previous studies showing that the larger the mangrove width, the better the protection offered by  
98 mangroves against waves (e.g., Barbier et al., 2008). However, this finding is pertinent to wave energy  
99 being dissipated across a more or less broad mangrove belt, which is not quite the same thing as  
100 mangrove protection against an ongoing erosion process. Furthermore, an environment for successful  
101 mangrove seedling requires that substrate accretion levels are maintained by sustained sediment supply  
102 (Balke et al., 2011).

103  
104 The objective of this paper is to further test the relationship described by Phan et al. (2015) based  
105 on the rationale that the shoreline change trends deduced from satellite images in recent studies may be  
106 correlated with mangrove width identified on the same satellite images. We first compare mangrove  
107 width and shoreline change over cross-shore profiles at the scale of the entire delta, then at the scale of  
108 the three deltaic sectors commonly identified along the Mekong delta (e.g., Anthony et al., 2015): the  
109 delta distributary mouths sector (0-280 km), the ‘East Coast’ (280-379 km) bordering the South Sea, and  
110 the ‘West Coast’ in the Gulf of Thailand (379-564 km) (Fig. 1). Following this, we gauged the  
111 relationship between mangroves and shoreline change in the delta.

## 113 2. Data and Methods

### 114 2.1 Remote-sensing data

115 Using a relevant cartographic frame (Projection UTM 48N), a baseline  $B$  was set about 1 km  
116 offshore (Fig. 2) of the Mekong delta shoreline. This baseline was regular enough to: (i) smooth any  
117 small-scale instabilities related to a non-rectilinear shoreline, and (ii) delineate large-scale geomorphic  
118 features such as capes or bays. We then set up regularly spaced transects perpendicular to the baseline  
119 and extending from offshore to 3 kilometres inland. Following this, we projected a set of 43 high-  
120 resolution SPOT 5 level 3 ortho-rectified colour satellite images for January 2003 (2003) and December  
121 2011/February 2012 (2012) at a scale of 1:10,000 within the cartographic frame. These images, initially  
122 described in Anthony et al. (2015), cover the  $\approx 500$  km of delta shoreline. The SPOT 5 images are 5 m  
123 pixel-resolution panchromatic images (spectral band within 0.48-0.71  $\mu\text{m}$ ) acquired in pairs  
124 simultaneously with a half-pixel spatial shift. The resulting SPOT 5 Super-Mode images offer a final  
125 resolution of 2.5 m appropriate for precisely locating the shorelines and the edges of the mangrove fringe.  
126 This is the best theoretical spatial resolution for the study.

### 127 2.2. Extraction of shorelines and mangrove limits

128 There is no standardized definition of the shoreline (e.g., Boak and Turner, 2005; Ruggiero and  
129 List, 2009) and this implies the choice of a yardstick, preferably one that can be re-used in successive  
130 surveys, to identify a position of the land-water interface. Following extensive field observations  
131 covering over 300 km of the Mekong delta's shoreline over the period 2011-2012, Anthony et al. (2015)  
132 suggested the use of the seaward limit of vegetation as the shoreline. The brush/plantation fringe in  
133 sectors of sandy coast characterized by beaches, and the mangrove fringe in the muddy sectors, were  
134 adopted as good 'shoreline' markers. We used the shoreline digitized in Anthony et al. (2015) from the  
135 2003 and 2012 images using the automatic digital shoreline analysis DSAS (Himmelstoss et al., 2018),  
136 and traced 4155 new cross-shore transects, spaced 100 m alongshore. This alongshore spacing appeared  
137 to provide the best compromise between precision and the overall length of analyzed delta shoreline (415  
138 km). Phan et al. (2015) selected a set of only 18 transects to define the relationship between mangrove  
139 width and shoreline change over the period 1989-2002. Our study is based on the systematic analysis of a  
140 much larger set of transects but also concerns a more recent period marked by increasing erosion of the  
141 delta (Anthony et al., 2015; Li et al., 2017). Transects through mangrove vegetation were retained as the  
142 primary basis for our analysis. It may be noted that at least half of the transects used by Phan et al. (2015)  
143 could not have concerned mangrove-bearing shorelines since they went through sandy (open beach-  
144 foredune) portions of the river-mouth sector (see their Fig. 1B). 45% (113 km out of 250 km) of the  
145 delta's shoreline is characterized by 'upland' brush-plantation vegetation associated with these beaches  
146 and foredunes in the river-mouth sector (Anthony et al., 2015). We digitized the inland limit of the  
147 mangrove fringe using the same procedure as Phan et al. (2015). This consisted in using dikes observed  
148 on satellite images as this inland limit (Fig. 2).

149 Along each cross-shore transect superimposed on these images, we digitised the following curves:

150 •  $S_{2003}$ : the shoreline in 2003,

151 •  $S_{2012}$ : the shoreline in 2012,

152 •  $M_{inland}$ : the line defining the 2012 inland limit of vegetation up to the main dike,

153 •  $M_{shore}$ : the line defining the 2012 seaward limit of vegetation.

154 Since the issue at hand here is simply that of determining the relationship between the width of a  
155 mangrove fringe at a time  $t$  with shoreline change over several years, we had a choice between the 2003  
156 and 2012 satellite images. The results yielded by the two datasets are virtually identical (Supplementary  
157 Material 1). We preferred, thus, the 2012 images which are of better quality than those of 2003,  
158 especially for delimiting the landward vegetation fringe, and the comparison is coherent with that  
159 adopted by Phan et al. (2015).

160 We extracted the positions of the four digitized lines at the intersection with each cross-shore  
161 profile. Thus, in the cartographic frame, we obtained four sets of shorelines and limits of mangroves:  
162  $(X_{2003}^i; Y_{2003}^i)_{i \in [1:N]}$ ,  $(X_{2012}^i; Y_{2012}^i)_{i \in [1:N]}$ ,  $(X_{inland}^i; Y_{inland}^i)_{i \in [1:N]}$ , and  $(X_{shore}^i; Y_{shore}^i)_{i \in [1:N]}$  where  $i$   
163 refers to a cross-shore profile and  $N$  is the total number of cross-shore profiles. In addition, we obtained  
164 the set  $(X_B^i; Y_B^i)_{i \in [1:N]}$  of node coordinates along the baseline from which each cross-shore transect  
165 commences.

166 Using these five datasets, we determined the following distances to the baseline:

167 • the distance of the 2003 shoreline

$$168 \quad S_{2003}^i = \sqrt{(X_{2003}^i - X_B^i)^2 + (Y_{2003}^i - Y_B^i)^2} \quad (1)$$

169 • the distance of the 2012 shoreline

$$170 \quad S_{2012}^i = \sqrt{(X_{2012}^i - X_B^i)^2 + (Y_{2012}^i - Y_B^i)^2} \quad (2)$$

171 • the distance of the 2012 inland edge of the mangrove fringe

$$172 \quad M_{inland}^i = \sqrt{(X_{inland}^i - X_B^i)^2 + (Y_{inland}^i - Y_B^i)^2} \quad (3)$$

173 • the distance of the 2012 seaward edge of the mangrove fringe

174 
$$M_{shore}^i = \sqrt{(X_{shore}^i - X_B^i)^2 + (Y_{shore}^i - Y_B^i)^2} \quad (4)$$

175 We calculated the mean annual rate of shoreline change  $V_S^i$  at each cross shore transect  $i$ :

176 
$$V_S^i = \frac{S_{2003}^i - S_{2012}^i}{\Delta T} \quad (5)$$

177 where  $\Delta T$  is the time interval between the two consecutive SPOT 5 surveys (9 years). We also  
 178 calculated the current width of the mangrove fringe  $W^i$  at each cross-shore transect  $i$ :

179 
$$W^i = M_{inland}^i - M_{shore}^i \quad (6)$$

180 Following these procedures, we carried out analysis of possible relationships between  $V_S^i$  and  $W^i$   
 181 at various spatial scales, by considering various subsets of cross-shore transects. A few stretches of  
 182 shoreline (less than 5% overall) could not be analyzed because of various technical problems such as  
 183 cloud cover, thin (< 10 m wide) residual mangrove fringe, or where the edge of mangroves was not  
 184 readily distinguishable on the images. Finally, taking into account these limitations, we obtained 3687  
 185 relevant pairs of shoreline change ( $V^i$ ) and mangrove width ( $W^i$ ).

186

### 187 **2.3. Error margins and uncertainty**

188 Anthony et al. (2015) demonstrated that a good estimate of  $E_V$ , the mean uncertainty for  $V^i$ , is of  
 189 the order of  $\pm 5$  m/yr for all of the cross-shore transects. In this paper, we needed to define the margin of  
 190 error in the quantification of  $W^i$ . To do so, we considered  $E_p$  [m], the total error in the positioning of the  
 191 points defining mangroves inland and the limits of the shore (Fletcher et al., 2003; Rooney et al., 2003;  
 192 Hapke et al., 2006):

193 
$$E_p = E_r^2 + E_g^2 + E_c^2 \quad (7)$$

194 The three mean squared errors are relative to: (i)  $E_r$  [m] the image resolution, (ii)  $E_g$  [m] the SPOT  
 195 5 georeferencing, and (iii)  $E_c$  [m] the size of the cursor used to digitize the mangrove fringe line (which  
 196 depends on the scale at which the image is plotted during digitizing). Fletcher et al. (2003), Rooney et al.  
 197 (2003), and Hapke et al. (2006) considered tidal fluctuations as a possible alternative source of  
 198 uncertainty in  $E_p$ . To handle this problem, we checked that the SPOT 5 images in 2012 were shot more  
 199 or less at the same moment in the tidal cycle. Thus, this contribution remains very negligible and was not  
 200 considered further in this study.

201 Practically,  $E_c$  was set to 2.8 m precisely for the study.  $E_g$  varied from 1.4 to 2.9 m.  $E_r$  was 2.5 m  
 202 as explained above. As a consequence, we had a mean positioning uncertainty  $E_p$  ranging from 4.0 to 4.7  
 203 m. We considered this margin of error as constant throughout for all the 3687 profiles. Finally, we  
 204 calculated  $E_W$ [m] the mean uncertainty for the mangrove fringe widths  $W^i$  for all the transects as being  
 205 the quadratic error of positioning at the inland and seaward limits of the mangrove fringe:

$$206 \quad E_W = \frac{1}{N} \sum \left( \sqrt{E_{inland}^2 + E_{shore}^2} \right) \quad (8)$$

207 where  $E_{inland}$  is the positioning error defined for the inland limit of the mangrove width and  
 208  $E_{shore}$  that of the seaward limit. As the SPOT 5 images are the same for seaward and inland limit  
 209 digitizing,  $E_{inland} = E_{shore}$ , which meant that:

$$210 \quad E_W = \frac{\sqrt{2}}{N} \sum_1^N E_p \quad (9)$$

211

### 212 3. Results

213 The statistical comparison between shoreline change and coastal mangrove width is carried out at  
 214 two scales: regional and local.

#### 215 3.1 Regional scale (river-mouths/East Coast/West Coast)

216 When all 3687 transects are considered, there are no statistical correlations at the larger, regional  
 217 scale (Fig. 4). 31% ( $\approx 80$  km) of eroded shorelines are bordered by a mangrove width larger than the  
 218 upper limit of a 500 m-wide mangrove fringe proposed by Phan et al. (2015) to ensure sediment trapping.  
 219 Delimiting a threshold is difficult when all the data are taken into account without sorting. We therefore  
 220 resorted to discretization and ranking of the results.

221 The results obtained thus show a decline in the number of cross-shore eroding transects as the  
 222 width of the mangrove fringe increases (Fig. 4). In the delta distributary mouths, a decrease in the  
 223 proportion of eroding transects in favour of that of prograding transects is observed, with mangrove  
 224 width increasing until a threshold of 400 m. In this sector, only 8.5% (116 out of the 1370 profiles) of the  
 225 shoreline shows a direct linear relationship between mangrove width and the rate of erosion/accretion.

226 Along the East and West Coasts, no trend comes out, the percentage of transects in erosion varying  
 227 only slightly as a function of mangrove width (Fig. 4B). In fact, the number of erosional transects along  
 228 the East Coast increases despite large mangrove widths, whereas the number of those in the mouths  
 229 sector and the West Coast decrease (i.e. 0.6–1.2 km-wide mangrove). The results also show that the East

230 Coast is largely dominated by erosion (97% of black dots in Fig. 3), even though the width of the  
231 mangrove belt exceeds 2 km in places.

### 232 **3.2 Local scale (5 km-long transects)**

233 To go further into the analysis, we divided the shoreline into longshore segments of 5 km (50  
234 consecutive transects) (Fig. 5). At this scale, we integrated transects with non-mangrove vegetation at the  
235 delta distributary mouths. Each line in the figure represents a coastal segment where a linear trend is  
236 observed. Along the 482 km of shoreline analyzed (including 113 km of shoreline with ‘upland’ brush-  
237 plantation vegetation), we identified only nine segments of deltaic shoreline, exclusively in the mouths  
238 sector and the West Coast, showing a significant relationship ( $r^2 > 0.75$ , up to 1) between mangrove width  
239 and shoreline change (Fig. 5). Each segment has an alongshore length ranging from 0.5 to 5 km (5 to 50  
240 consecutive points separated 100 m alongshore are aligned in Fig. 3). These segments represent a  
241 cumulative length of 37 km, i.e.  $\approx 10\%$  of the total length of analyzed shoreline. Of this, 16.6 km  
242 correspond to shoreline segments with non-mangrove vegetation.

243

## 244 **4. Discussion**

245 At the overall regional scale, our results reveal a pattern that is more complex than the simple  
246 linear relationship proposed by Phan et al. (2015) between mangrove width and the status of the shoreline  
247 in the Mekong delta. The results obtained in the present study, and based on a comprehensive analysis of  
248 3687 pairs of shoreline change and mangrove width spaced 100 m (i.e., covering a total shoreline length  
249 of 369 out of ca. 500 km of delta shoreline), show no statistically significant relationships, whatever the  
250 scale considered (Figs. 3, 4, 5). This goes with the field observations of Anthony et al. (2015) who  
251 reported active and quasi-continuous alongshore erosion of muddy mangrove-bearing bluffs along much  
252 of the East and West Coasts in 2012. Two immediate inferences that come out of these findings are: (1)  
253 that a large mangrove width is not necessarily tantamount to shoreline progradation in the Mekong delta;  
254 (2) the overarching role of prevailing erosion which, where established, leads to sustained shoreline  
255 retreat, whatever the width of the mangrove belt. There is no doubt that mangroves, by dissipating waves  
256 and currents, can contribute actively to protection of a variably wide coastal fringe (which is not quite the  
257 same thing as protection of the shoreline on which waves impinge), and can, especially, promote rapid  
258 coastal accretion where fine-grained sediment supply is adequate, or delay, but not halt, coastal retreat,  
259 where the sediment supply is inadequate. Our study shows, however, that for  $\approx 90\%$  of the Mekong delta  
260 shoreline, the relationship between mangroves and how the shoreline evolves needs to be carefully  
261 considered in a context that takes into account antecedent and prevailing shoreline erosion or accretion.  
262 These situations of erosion or accretion are, in turn, vested in the larger-scale control exerted by  
263 alongshore adjustments between net sediment supply or availability, wave and current energy, and  
264 sediment redistribution by waves and currents (Anthony et al., 2015; Marchesiello et al., 2019). Ignoring

265 these basic aspects may imply that high expectations from mangroves could be met with disappointment.  
266 This can have important shoreline management implications because of the following wrong deductions:  
267 (1) a large mangrove fringe is enough to stabilize a (eroding) shoreline, (2) some reduction of the  
268 mangrove width to the benefit of other activities such as shrimp-farming is not deleterious, and (3) the  
269 effects of human-induced reductions in sediment supply to the coast can be offset by mangroves.

270 The foregoing points simply warn that the efficiency of mangroves in assuring shoreline stability  
271 needs to be viewed in the light of the established (decadal) shoreline trend, which, in turn, is determined  
272 by sediment supply and hydrodynamic conditions. The protective capacity of mangroves can be  
273 particularly impaired where sediment supply is in strong or persistent deficit, fine examples being the  
274 mangrove-rich Guianas coast between the Amazon and Orinoco river mouths, the world's longest muddy  
275 coast (Anthony and Gratiot, 2012). Here, so-called decadal to multi-decadal 'inter-bank' phases of  
276 relative mud scarcity separating mud-rich 'bank' phases (discrete mud banks migrating alongshore from  
277 the mouths of the Amazon are separated by inter-bank zones of erosion) can be characterized by rates of  
278 shoreline erosion that can exceed 150 m/year notwithstanding the presence of dense mangrove forests up  
279 to 30 m high and forming stands several km-wide (Brunier et al., 2019).

280 The width of the energy-dissipating mangrove fringe alone does not play a determining role,  
281 neither in the context of erosive oceanic forcing, nor in the context of decreasing sediment supply to the  
282 delta. This reflects a tipping-point effect wherein once sediment supply to the coast is in chronic deficit (a  
283 deficit aggravated by delta-plain trapping to compensate for accelerated subsidence), the vertical growth  
284 of shorefront mudflats is no longer assured. Mangrove colonization can be precluded where shorefront  
285 mudflat elevations are below a tidal level threshold to enable seedling establishment (Proisy et al., 2009;  
286 Balke et al., 2011, 2013). Shorefront substrate elevations in the Mekong delta have not been monitored,  
287 but these unfavourable conditions for mangroves are likely exacerbated by: (1) narrowing of the  
288 mangrove fringe which entails less wave dissipation and therefore decrease in turbulence dissipation and  
289 flocculation (Gratiot et al., 2017); and (2) the increasing number of aquaculture farms and dykes to  
290 protect rice farms, limiting the tidal prism with negative effects on sediment trapping (Li et al., 2017). At  
291 the local scale of a few km, increasing mangrove width can be correlated with shoreline change, as at km  
292  $\approx 455$  in the southern extremity of the delta, near Ca Mau point (Fig. 1), where there appears to be  
293 convergence of suspended mud (Marchesiello et al., 2019). Hence, the pertinence of a comparative  
294 analysis at different scales (local/individual transects, alongshore segments, delta mass as a whole  
295 representing the entire river basin).

296 Reflections on coastal management and coastal protection measures adapted to the Mekong delta  
297 imply acquiring a good grasp of the resilience of the delta's mangroves. Efforts aimed jointly at  
298 maintaining and preserving, rather than further destroying, mangroves (Jhaveri and Nguyen, 2018;  
299 Veettil et al., 2019), and in assuring sustained sediment supply to the delta shores, will also be required in  
300 the years to come.

301

302 **5. Conclusions**

303 1. The width of the mangrove fringe rimming 369 km ( $\approx 90\%$ ) of the Mekong delta shoreline, and  
304 shoreline change between 2003 and 2012, were determined for 3687 cross-shore transects spaced 100 m  
305 apart from a comparison of high-resolution satellite images. The results show that 68% of the delta  
306 shoreline is undergoing erosion and 91% of the eroding shoreline is characterized by mangroves.

307 2. Statistical relationships between shoreline change and mangrove width were determined: (a) at  
308 the scale of the entire dataset of 3687 transects, (b) at the scale of the three sectors composing the delta  
309 shoreline: the delta distributary mouths, dominantly characterized by sandy beach-dune shorelines, and  
310 which was therefore largely excluded from this analysis, and the muddy East and West coasts, hitherto  
311 rich in mangroves, and, (c) at a more local level comprised of transects over shoreline segments of 5 km.

312 3. The results show no significant trend, whatever the level considered. This finding differs from  
313 that of Phan et al. (2015) who depicted, on the basis of only 18 data points, a linear relationship between  
314 reduced mangrove width and coastal erosion. A linear relationship was observed in a very few sectors  
315 accounting for less than 5.5% of the entire delta shoreline.

316 4. Phan et al. (2015) identified a minimum critical width of 140 m for a stable mangrove fringe, and  
317 above this width, a capacity for mangroves to promote sedimentation. Although a wide and healthy  
318 mangrove fringe is desirable, the 140 m-width recommended by Phan et al. (2015) is not a scientifically  
319 defensible width.

320 5. Our results indicate that the role of mangroves in coastal protection needs to be carefully  
321 considered in a context that takes into account antecedent prevailing shoreline erosion or accretion vested  
322 in the larger-scale alongshore adjustments between net sediment supply and the ambient coastal  
323 dynamics driven by waves and currents.

324 6. Beyond a certain threshold of deficient mud supply, and under maintained ambient  
325 hydrodynamic conditions, mangroves, whatever their width, can no longer assure shoreline advance or  
326 even stability, although they contribute to the attenuation of erosion by waves and currents.

327 7. Although erosion of mangrove-colonized shorelines results from natural morpho-sedimentary  
328 adjustments driven by sediment supply and hydrodynamic forcing, mangroves can contribute actively to  
329 coastal protection even under a context of shoreline erosion. Mangrove removal contributes, thus, to the  
330 aggravation of shoreline erosion.

331 8. Reflections on coastal protection in the Mekong delta require not only a good knowledge of the  
332 resilience of mangroves, efforts aimed at preserving them, but also understanding the large-scale

333 processes (source-to-sink sediment supply, oceanic forcing, climate change) that assure sustained  
334 sediment supply to the delta shores, building and maintaining the delta in a dynamic equilibrium.

335

336

### 337 **Acknowledgements**

338 We acknowledge initial joint funding from Fond Français pour l'Environnement Mondial (FFEM)  
339 and WWF Greater Mekong. Further support was provided by the ANR-Belmont Forum Project 'BF-  
340 Deltas: Catalyzing Action Towards Sustainability of Deltaic Systems with an Integrated Modeling  
341 Framework for Risk Assessment', and by the Lower Mekong Delta Coastal Zone project (LMDCZ, EU-  
342 AFD & SIWRR, 2018). The SPOT 5 images were provided by the CNES/ISIS programme (© CNES  
343 2012, distribution Spot Image S.A.). We thank two anonymous reviewers for their insightful comments  
344 and suggestions. We thank Colin Woodroffe and an anonymous reviewer for their insightful comments  
345 and suggestions.

346

### 347 **References**

348 Albers, T., Schmitt, K., 2015. Dyke design, floodplain restoration and mangrove co-management  
349 as parts of an area coastal protection strategy for the mud coasts of the Mekong delta, Vietnam. *Wet.*  
350 *Ecol. Manag.*, 23, 6, 991–1004. <https://doi.org/10.1007/s11273-015-9441-3>

351 Allison, M.A., Nittrouer C.A., Ogston, A.S., Mullarney, J.C., Nguyen, T.T, 2017. Sedimentation  
352 and survival of the Mekong Delta: A case study of decreased sediment supply and accelerating rates of  
353 relative sea level rise. *Oceanography* 30, 98–109, <https://doi.org/10.5670/oceanog.2017.318>.

354 Alongi, D.M., 2008. Mangrove forests: Resilience, protection from tsunamis, and responses to  
355 global climate change. *Estuar. Coast. Shelf Sci.*, 76, 1, 1 - 13. <https://doi.org/10.1016/j.ecss.2007.08.024>

356 Anthony, E.J., 2004. Sediment dynamics and morphological stability of an estuarine mangrove  
357 complex: Sherbro Bay, West Africa. *Mar. Geol.*, 208, 207-224.

358 Anthony, E.J., Brunier, G., Besset, M., Goichot, M., Dussouillez, P., Nguyen, V.L., 2015. Linking  
359 rapid erosion of the Mekong River delta to human activities. *Sci. Rep.*, 5, 1–12.  
360 <http://dx.doi.org/10.1038/srep14745>

361 Anthony, E.J., Gratiot, N., 2012. Coastal engineering and large-scale mangrove destruction in  
362 Guyana, south America: Averting an environmental catastrophe in the making. *Ecol. Eng.*, 47, 268 - 273.  
363 <https://doi.org/10.1016/j.ecoleng.2012.07.005>

364 Balke, T., Bouma, T.J., Horstman, E.M., Webb, E.L., Erfteimeijer, P.L.A., Herman, P.M.J., 2011.  
365 Windows of opportunity: thresholds to mangrove seedling establishment on tidal flats. *Marine Ecological*  
366 *Progress Series*, 440, 1–9.

367 Balke, T., Webb, E.L., van den Elzen, E., Galli, D., Herman, P.M.J., Bouma, T.J., 2013. Seedling  
368 establishment in a dynamic sedimentary environment: a conceptual framework using mangroves. *J. Appl.*  
369 *Ecol.*, 50, 740–747.

370 Barbier, E.B., Koch, E.W., Silliman, B.R., Hacker, S.D., Wolanski, E., Primavera, E.J., Granek,  
371 E.F., Polasky, S., Aswani, S., Cramer, L.A., Stoms, D.M., Kennedy, C.J., Bael, D., Kappel, C.V., Perillo  
372 G.M.E., Reed, D. 2008. Coastal ecosystem based management with non-linear ecological functions and  
373 values. *Science*, 319, 321.

374 Besset, M., Anthony, E.J., Brunier, G., Dussouillez, P., 2016. Shoreline change of the Mekong  
375 River delta along the southern part of the South China Sea coast using satellite image analysis (1973-  
376 2014). *Géomorphologie*, 22, 2, 137-146. <http://dx.doi.org/10.4000/geomorphologie.11336>

377 Boak, E.H., Turner, I.L., 2005. Shoreline definition and detection: A review. *Journal of Coastal*  
378 *Research*, 21, 688-703.

379 Boateng, I., 2012. GIS assessment of coastal vulnerability to climate change and coastal adaption  
380 planning in Vietnam. *J. Coast. Conserv.*, 16, 1, 25–36. <https://doi.org/10.1007/s11852-011-0165-0>

381 Brander, L.M., Wagtendonk, A.J., Hussain, S.S., McVittie, A., Verburg, P.H., Groot, R.S., Ploeg,  
382 S., 2012. Ecosystem service values for mangroves in Southeast Asia: a meta-analysis and value transfer  
383 application. *Ecosyst. Serv.*, 1, 62–69. <https://doi.org/10.1016/j.ecoser.2012.06.003>.

384 Brunier, G., Anthony, E.J., Gratiot, N., Gardel, A., 2019. Exceptional rates and mechanisms of  
385 muddy shoreline retreat following mangrove removal. *Earth Surf. Process. Landf.*,  
386 <https://doi.org/10.1002/esp.4593>.

387 Carlton, J.M., 1974. Land-building and stabilization by mangroves. *Environ. Conserv.*, 1, 4,  
388 285-294. <https://doi.org/10.1017/S0376892900004926>

389 Christensen, S.M., Tarp, P., Hjortso, C.N., 2008. Mangrove forest management planning in coastal  
390 buffer and conservation zones, Vietnam: A multimethodological approach incorporating multiple  
391 stakeholders. *Ocean Coast. Manag.*, 51, 10, 712 - 726. <https://doi.org/10.1016/j.ocecoaman.2008.06.014>

392 Coleman, M., Huh, O.K., 2004. Major deltas of the world: A perspective from space. *Coastal*  
393 *Studies Institute, Louisiana State University, Baton Rouge, LA.*  
394 ([www.geol.lsu.edu/WDD/PUBLICATIONS/CandHnasa04/CandHfinal04.htm](http://www.geol.lsu.edu/WDD/PUBLICATIONS/CandHnasa04/CandHfinal04.htm).)

395 Corenblit, D., Tabacchi, E., Steiger, J., Gurnell, A.M., 2007. Reciprocal interactions and  
396 adjustments between fluvial landforms and vegetation dynamics in river corridors: A review of  
397 complementary approaches. *Earth Sci. Rev.*, 84, 1, 56 - 86.  
398 <https://doi.org/10.1016/j.earscirev.2007.05.004>

399 Doody, J.P., 2004. ‘Coastal squeeze’: An historical perspective. *J. Coast. Conserv.*, 10, 1-2, 129–  
400 138. <http://www.jstor.org/stable/25098445>

401 Fletcher, C., Richmond, B., Rooney, J., Barbee, M., Lim, S.C., 2003. Mapping shoreline change  
402 using digital orthophotogrammetry on Maui, Hawaii. *J. Coast Res.*, SI 38, 106–124.  
403 <https://www.jstor.org/stable/25736602>

404 Furukawa, K., Wolanski, E., Mueller, H., 1997. Currents and sediment transport in mangrove  
405 forests, *Estuarine, Coast. Shelf Sci.*, **44**, 3, 301. <https://doi.org/10.1006/ecss.1996.0120>

406 Gedan, K.B., Kirwan, M.L., Wolanski, E., Barbier, E.B., Silliman, B.R., 2011. The present and  
407 future role of coastal wetland vegetation in protecting shorelines: answering recent challenges to the  
408 paradigm. *Clim. Change*, 106, 1, 7–29. <https://doi.org/10.1007/s10584-010-0003-7>

409 General statistics office of Vietnam. statistical data., 2015.  
410 [https://www.gso.gov.vn/Default\\_en.aspx?tabid=491](https://www.gso.gov.vn/Default_en.aspx?tabid=491). (Accessed: 1 April 2015)

411 Gilman, E., Ellison, J., Coleman, R., 2007. Assessment of mangrove response to projected relative  
412 sea-level rise and recent historical reconstruction of shoreline position. *Environmental Monitoring and*  
413 *Assessment*, 124, 1, 105–130. <https://doi.org/10.1007/s10661-006-9212-y>

414 Gilman, E.L., Ellison, J., Jungblut, V., Van Lavieren, H., Wilson, L., Areki, F., Brighthouse, G,  
415 Bungitak, J, Dus, E, Henry, M, Kilman, M, Matthews, E., 2006. Adapting to Pacific Island mangrove  
416 responses to sea level rise and climate change. *Clim. Res.*, 32, 3, 161–176.  
417 <https://doi.org/10.3354/cr032161>

418 Gratiot, N., Bildstein, A., Anh, T.T., Thoss, H., Denis, H., Michallet, H. and Apel, H., 2017.  
419 Sediment flocculation in the Mekong river estuary, Vietnam, an important driver of geomorphological  
420 changes. *Comptes rendus Geosciences*, 349 (6), 260-268.

421 Gupta, A., 2009. Chapter 3 - geology and landforms of the Mekong basin. In I.C. Campbell (Ed.),  
422 *The Mekong: Biophysical Environment of an International River Basin* (29 – 51). San Diego: Academic  
423 Press. <https://doi.org/10.1016/B978-0-12-374026-7.00003-6>

424 Ha, D.T., Ouillon, S. and Vinh, G.V. 2018. Water and suspended sediment budgets in the Lower  
425 Mekong from high-frequency measurements (2009-2016). *Water*, 10(7), 846.  
426 <https://doi.org/10.3390/w10070846>

427 Hapke, C.J., Reid, D., Richmond, B.M., Ruggiero, P., List, J., 2006. National Assessment of  
428 Shoreline Change Part 3: Historical Shoreline Change and Associated Coastal Land Loss Along Sandy  
429 Shorelines of the California Coast (Tech. Rep.). U.S. Geological Survey, 1219, 79 pp.

430 Hashim, A.M., Catherine, S.M.P., 2013. A laboratory study on wave reduction by mangrove  
431 forests. *APCBEE Procedia*, 5, 27 – 32. 4th International Conference on Environmental Science and  
432 Development ICESD. <https://doi.org/10.1016/j.apcbee.2013.05.006>

433 Heatherington, C., Bishop, M.J., 2012. Spatial variation in the structure of mangrove forests with  
434 respect to seawalls. *Mar. Freshwater Res.*, 63, 926–933. <https://doi.org/10.1071/MF12119>

435 Himmelstoss, E.A., Henderson, R.E., Kratzmann, M.G., and Farris, A.S., 2018, Digital Shoreline  
436 Analysis System (DSAS) version 5.0 user guide: U.S. Geological Survey Open-File Report 2018–1179,  
437 110 p., <https://doi.org/10.3133/ofr20181179>.

438 Horstman, E.M., Dohmen-Janssen, C.M., Narra, P.M.F., Van den Berg, N.J.F., Siemerink, M.,  
439 Hulscher, S.J.M.H., 2014. Wave attenuation in mangroves: a quantitative approach to field observations.  
440 *Coast. Eng.*, 94, 47–62. <https://doi.org/10.1016/j.coastaleng.2014.08.005>

441 Jhaveri, N., Nguyen, T.D., Nguyen, K.D., 2018. Mangrove collaborative management in Vietnam  
442 and Asia. USAID Report, 70 pp.

443 Kathiresan, K., 2003. How do mangrove forests induce sedimentation? *Revista de Biologia*  
444 *Tropical*, 51, 355–360.

445 Kéfi, S., Holmgren, M., Scheffer, M., 2016. When can positive interactions cause alternative stable  
446 states in ecosystems? *Funct. Ecol.*, 30, 1, 88-97. <https://doi.org/10.1111/1365-2435.12601>

447 Koehnken, L., 2014. Discharge Sediment Monitoring Project (DSMP) 2009 – 2013 Summary &  
448 Analysis of Results. Final Report, Mekong River Commission, Lao PDR, 126 pp.

449 Kumara, M.P., Jayatissa, L.P., Krauss, K.W., Phillips, D.H., Huxham, M., 2010. High mangrove  
450 density enhances surface accretion, surface elevation change, and tree survival in coastal areas  
451 susceptible to sea-level rise. *Oecologia*, 164, 2, 545–553. <https://doi.org/10.1007/s00442-010-1705-2>

452 Li, X., Liu, J.P., Saito, Y., Nguyen, V.L., 2017. Recent evolution of the Mekong delta and the  
453 impacts of dams. *Earth Sci. Rev.*, 175, 1 – 17. <https://doi.org/10.1016/j.earscirev.2017.10.008>

454 Marchesiello, P., Nguyen, N.M., Gratiot, N., Anthony, E.J., Nguyen, T., Almar, R., Kestenare, E.,  
455 2019. Erosion of the coastal Mekong delta: assessing natural against man induced processes. *Cont. Shelf*  
456 *Res.*, 181, 72-89. <https://doi.org/10.1016/j.csr.2019.05.004>

457 Marois, D.E., Mitsch, W.J., 2015. Coastal protection from tsunamis and cyclones provided by  
458 mangrove wetlands – a review. *Int. J. Biodiv. Sci., Ecosyst. Serv. Manag.*, 11, 71–83.

459 Massel, S., Furukawa, K., Brinkman, R., 1999. Surface wave propagation in mangrove forests.  
460 *Fluid Dyn. Res.*, 24, 4, 219 - 249. [https://doi.org/10.1016/S0169-5983\(98\)00024-0](https://doi.org/10.1016/S0169-5983(98)00024-0)

461 Mazda, Y., Magi, M., Kogo, M., Hong, P.N., 1997. Mangroves as a coastal protection from waves  
462 in the Tong king delta, Vietnam. *Mangroves Salt Marshes*, 1, 2, 127–135.  
463 <https://doi.org/10.1023/A:1009928003700>

464 McKee, K.L., Cahoon, D.R., Feller, I.C., 2007. Caribbean mangroves adjust to rising sea level  
465 through biotic controls on change in soil elevation. *Glob. Ecol. Biogeogr.*, 16, 5, 545-556.  
466 <https://doi.org/10.1111/j.1466-8238.2007.00317.x>

467 Mekong River Commission, 2010. State of the basin report. 123 pp. Vientiane, Lao PDR. ISBN  
468 978-993-2080-57-1

469 Minderhoud, P.S.J., Erkens, G., Pham, V.H., Bui, V.T., Erban, L., Kooi, H., Stouthamer, E., 2017.  
470 Impacts of 25 years of groundwater extraction on subsidence in the Mekong delta, Vietnam.  
471 *Environmental Research Letters*, 12, 064006.

472 Mitra, A., 2013. How mangroves resist natural disaster. In A. Mitra (Ed.), *Sensitivity of mangrove*  
473 *ecosystem to changing climate*. 107–129. Springer India.  
474 <https://books.google.fr/books?id=sXc8AAAAQBAJ>

475 Phan, L.K., van Thiel de Vries, J.S., Stive, M.J., 2015. Coastal mangrove squeeze in the Mekong  
476 delta. *J. Coast. Res.*, 233-243. <https://doi.org/10.2112/JCOASTRES-D-14-00049.1>

477 Phan, N.H., Hoang, T.S., 1993. *Mangroves of Vietnam*. 173 pp. IUCN, Bangkok. ISBN  
478 283170166X

479 Piman, T., Shrestha, M., 2017. *Case Study on Sediment in the Mekong River Basin: Current State*  
480 *and Future Trends*. UNESCO and Stockholm Environment Institute (SEI), 48 pp.

481 Pontee, N., 2013. Defining coastal squeeze: A discussion. *Ocean Coast. Manag.*, 84, 204 – 207.  
482 <https://doi.org/10.1016/j.ocecoaman.2013.07.010>

483 Proisy, C., Gratiot, N., Anthony, E.J., Gardel, A., Fromard, F., Heuret, P. 2009. Mud bank  
484 colonization by opportunistic mangroves: a case study from French Guiana using lidar data. *Continental*  
485 *Shelf Research*, 29, 632–641.

486 Quartel, S., Kroon, A., Augustinus, P., Santen, P.V., Tri, N., 2007. Wave attenuation in coastal  
487 mangroves in the red river delta, Vietnam. *Journal of Asian Earth Sciences*, 29 (4), 576 – 584.  
488 <https://doi.org/10.1016/j.jseaes.2006.05.008>

489 Rooney, J., Fletcher, C., Barbee, M., Eversole, D., Lim, S.-c., Richmond, B., Gibbs, A., 2003.  
490 *Dynamics of sandy shorelines in Maui, Hawaii - Soest Hawaii: Consequences and causes*. In *Coastal*  
491 *sediments (1–14)*. Florida.

492 Ruggiero, P., List, J.H., 2009. Improving accuracy and statistical reliability of shoreline position  
493 and change rate estimates. *Journal of Coastal Research*, 25, 1069-1081.

494 Torio, D.D., Chmura, G.L., 2013. Assessing coastal squeeze of tidal wetlands. *Journal of Coastal*  
495 *Research*, 29, 1049–1061.

496 Van Wesenbeeck, B., Balke, T., van Eijk, P., Tonneijck, F., Siry, H., Rudianto, M., Winterwerp, J.,  
497 2015. Aquaculture induced erosion of tropical coastlines throws coastal communities back into poverty.  
498 *Ocean and Coastal Management*, 116, 466 - 469. <https://doi.org/10.1016/j.ocecoaman.2015.09.004>

499 Veettil, B.K., Ward, R.D., Quangf, N.X., Trang, N.T.T., Giang, T.H., 2019. Mangroves of  
500 Vietnam: Historical development, current state of research and future threats. *Estuarine, Coastal and*  
501 *Shelf Science*, 218, 212-236. <https://doi.org/10.1016/j.ecss.2018.12.021>

502           Vidthayanon C. 2008. Field guide to fishes of the Mekong Delta. Mekong River Commission,  
503 Vientiane, Lao PDR. 288 pp.

504           Winterwerp, J.C., Erftemeijer, P.L.A., Suryadiputra, N., Van Eijk, P., Zhang, L., 2013. Defining  
505 eco-morphodynamic requirements for rehabilitating eroding mangrove-mud coasts. *Wetlands*, 33, 515–  
506 526.

507           Woodroffe, C., Rogers, K., McKee, K., Lovelock, C., Mendelssohn, I., and Saintilan, N., 2016.  
508 Mangrove sedimentation and response to relative sea-level rise. *Annual Review of Marine Science*, 8 (1),  
509 243-266. <https://doi.org/10.1146/annurev-marine-122414-034025>

510           World Wide Fund for Nature, 2012. Ecological footprint and investment in natural capital in Asia  
511 and the Pacific. ©Asian Development Bank and World-Wide Fund for Nature. CC BY-NC IGO 3.0. 104  
512 pp. <http://hdl.handle.net/11540/895>

513

514 **FIGURE CAPTIONS**

515

516 Figure 1. Map of the Mekong River delta showing shoreline change between 2003 and 2012 (from  
517 Anthony et al., 2015) in the three shoreline sectors: the sand-dominated delta distributary mouths, and the  
518 muddy East and West Coasts. Small rectangle on the East coast shoreline shows location of shoreline  
519 examples depicted in Fig. 2.

520 Figure 2. Examples of shorelines and positioning of the mangrove edge for digitization (see location in  
521 Fig. 1).

522 Figure 3. Graph showing the variation of Mekong delta shoreline change rates from 2003 to 2012 with  
523 mangrove width in 2012 (each dot corresponds to a transect), and discrimination of the three shoreline  
524 sectors (red dots for delta distributary mouths, black dots for East Coast, blue dots for West Coast). The  
525 six histograms show the frequency distribution for each sector with regards to mangrove width (left), and  
526 shoreline change (right).

527 Figure 4. Graphs showing the number (top) and the percentage (bottom) of transects in erosion among all  
528 transects in the different classes of 0.1 km mangrove-width range.

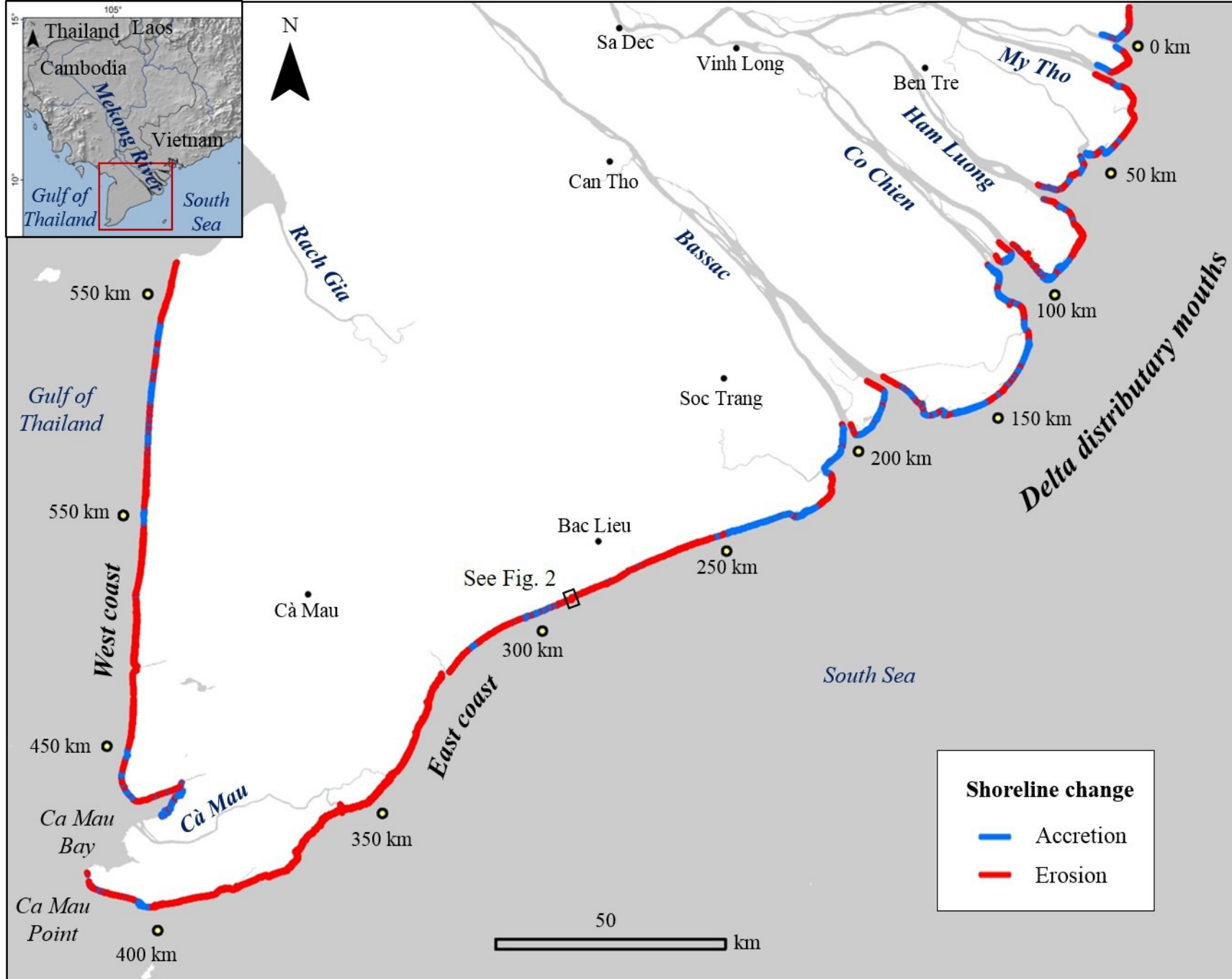
529 Figure 5. Locations of the 10% of shoreline sectors exhibiting a significant correlation between width of  
530 fringing vegetation and erosion/accretion. Of this, mangroves represent less than 5%.

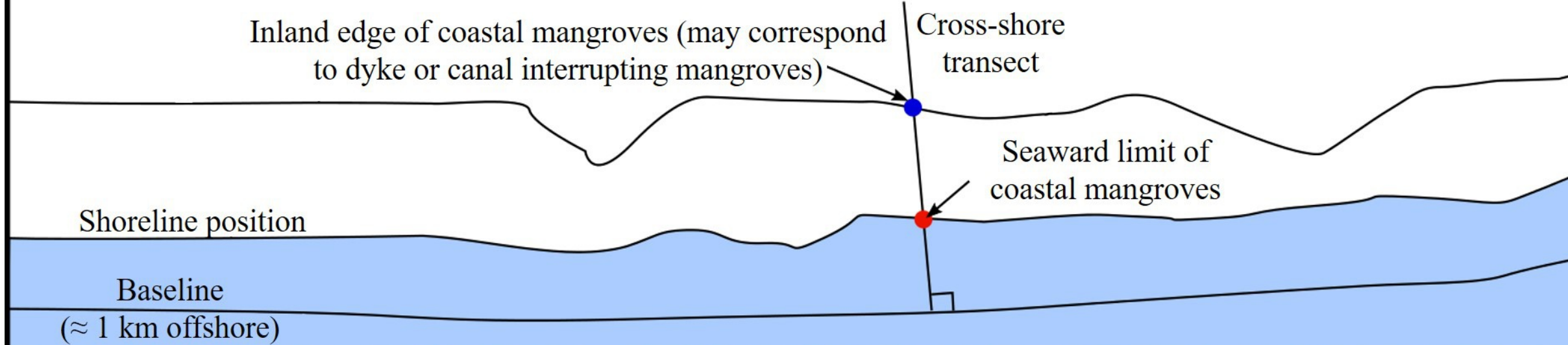
531

532 Supplementary material

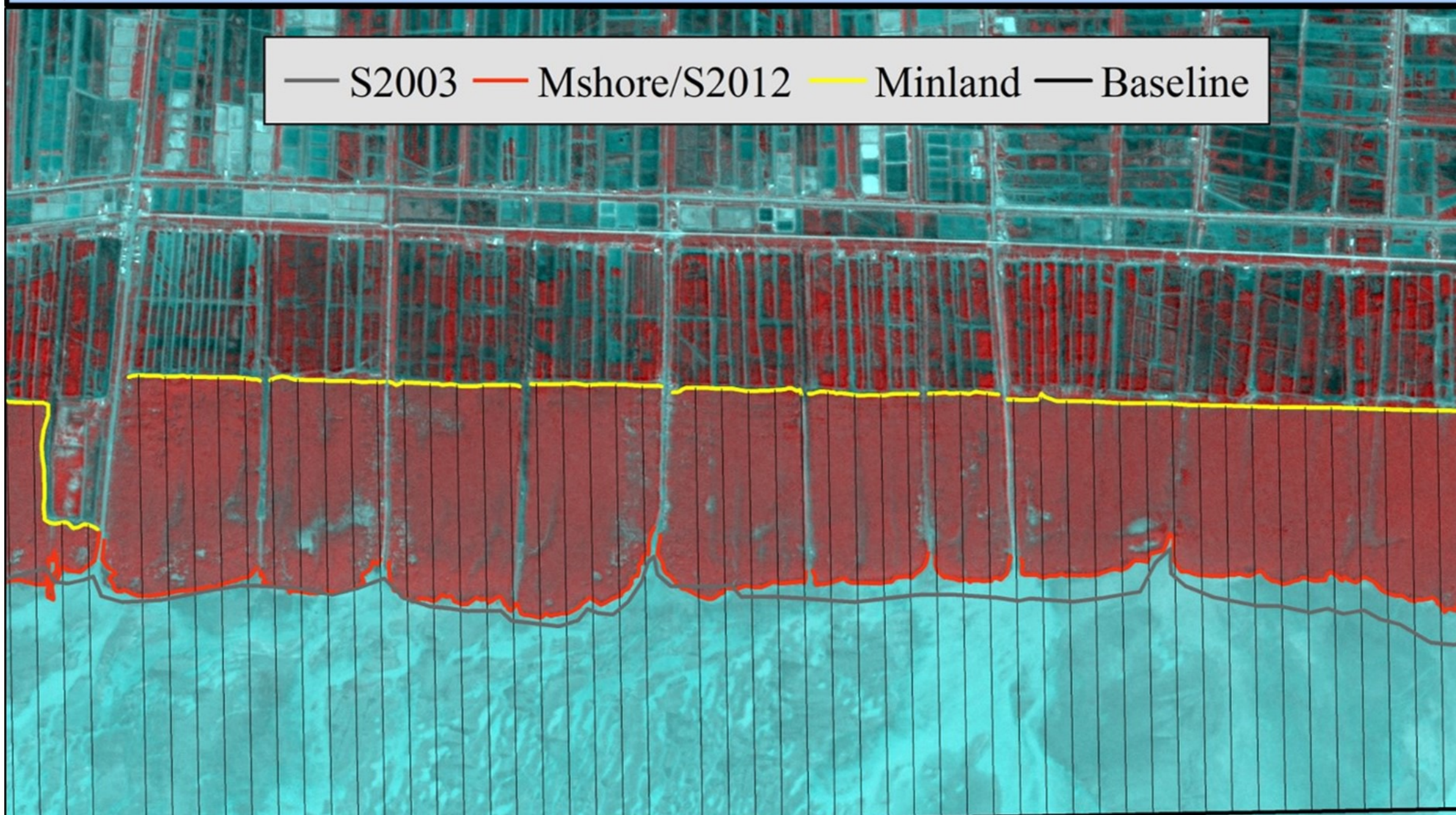
533 Comparison of the relationship between mangrove width and shoreline change based on the 2003 (a) and  
534 2012 (b) satellite images.

535

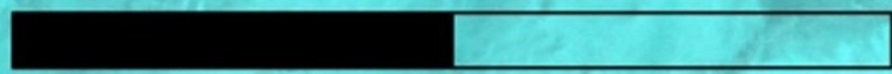


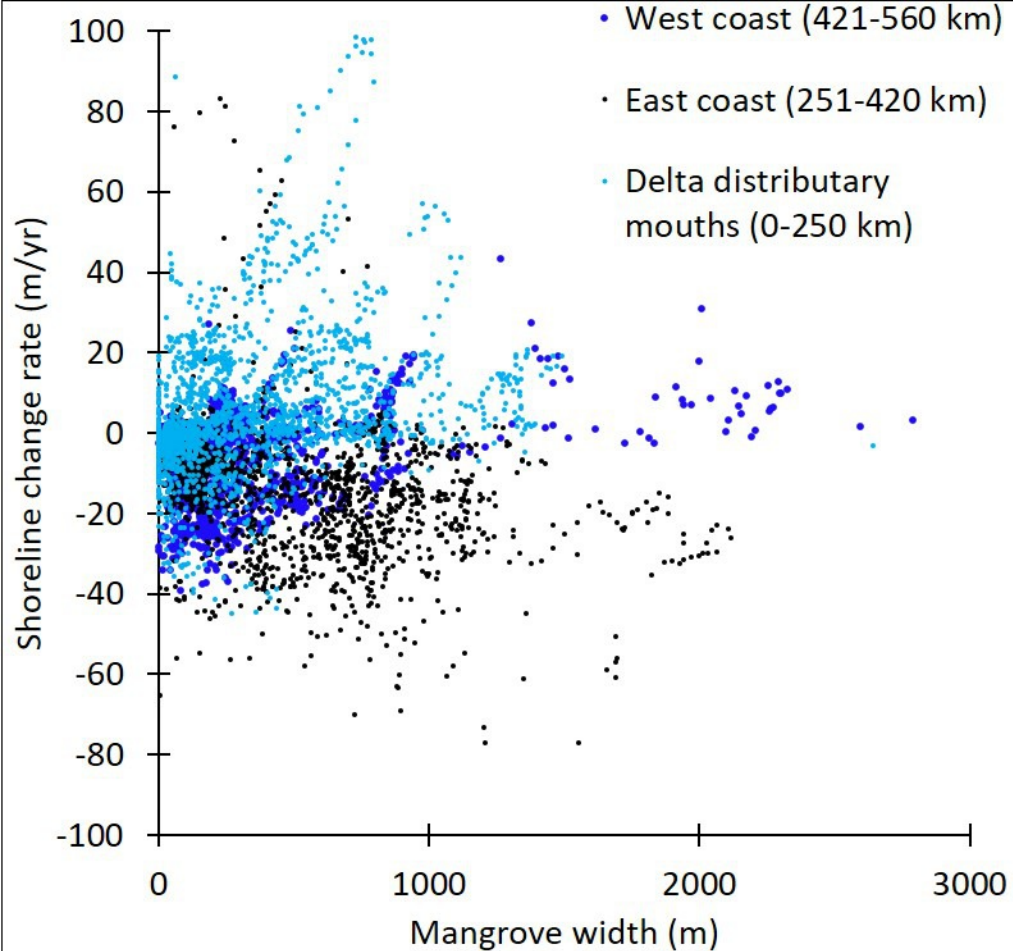


— S2003 — Mshore/S2012 — Minland — Baseline

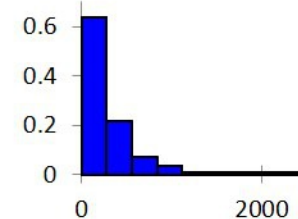
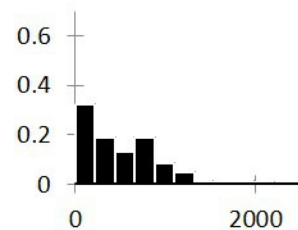
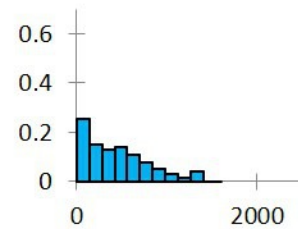


0 1 2 km

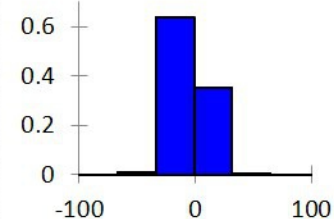
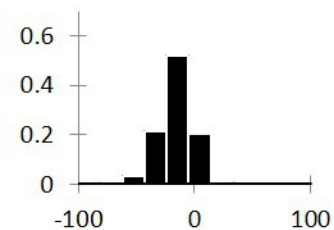
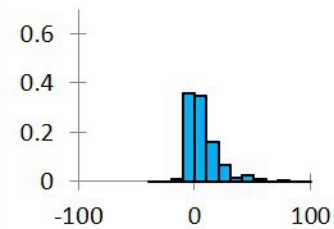


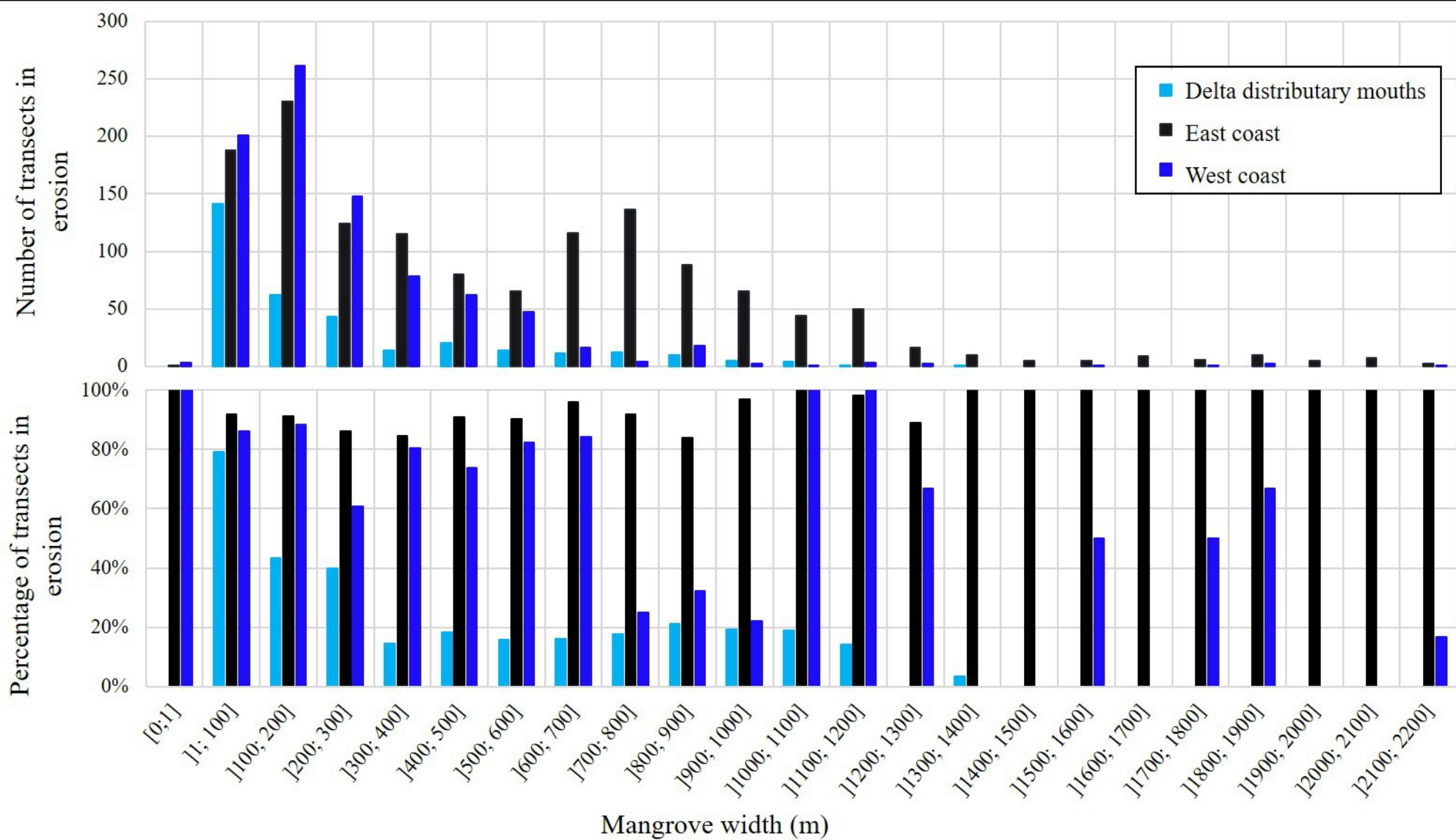


Mangrove width (m)

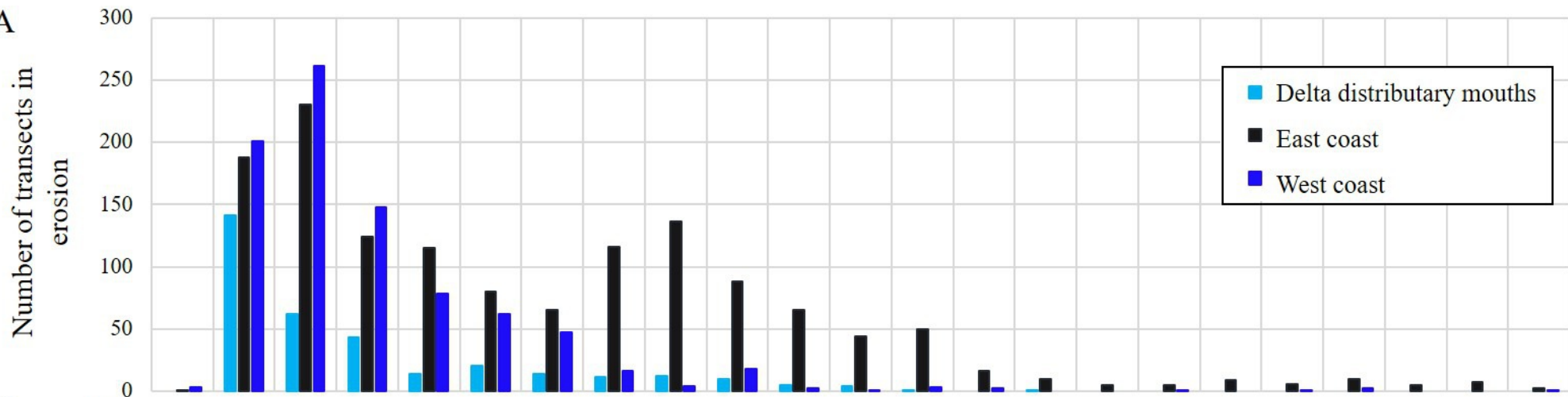


Shoreline change (m/yr)





A



B

